

# Layer-by-Layer Surface Modification and Patterned Electrostatic Deposition of Quantum Dots

Saeeda Jaffar,<sup>†</sup> Ki Tae Nam,<sup>‡,||</sup> Ali Khademhosseini,<sup>§,||</sup> Jia Xing,<sup>†</sup>  
Robert S. Langer,<sup>†,‡,§,||</sup> and Angela M. Belcher<sup>\*,‡,§,||</sup>

*Department of Chemical Engineering, Department of Materials Science and Engineering, Division of Biological Engineering, and Institute for Soldier Nanotechnologies, Massachusetts Institute of Technology, Cambridge, Massachusetts 02139-4307*

Received May 5, 2004

## ABSTRACT

Modification of ZnS-capped CdSe quantum dot (QD) surfaces with polyelectrolyte coatings and subsequent layer-by-layer deposition to build hierarchical structures are presented. Mercaptoacetic acid (MAA)-treated QDs were sequentially coated with polyallylamine (PAA) and polyvinylsulfonic acid (PVSA) and analyzed using zeta potentials, absorbance spectra, and transmission electron microscopy. The modified QDs were deposited on patterned hyaluronic acid (HA) glass substrates to produce self-assembled heterostructures (QDs-MAA/QDs-PAA/HA/glass), as revealed by fluorescence and atomic force microscopy.

Novel electroluminescent properties of quantum dots (QDs)<sup>1</sup> make them potential candidates for applications in photovoltaics,<sup>2</sup> multicolor LEDs,<sup>3</sup> electronic memory devices,<sup>4</sup> quantum dot barcodes,<sup>5</sup> and high throughput chemical<sup>6</sup> and biological sensors.<sup>7,8</sup> Before many applications can be realized, QDs must be functionally integrated into devices, which requires controlling their interactions with other materials and their spatial organization within a device.<sup>9</sup> Both may be achieved by manipulating their surface properties and engineering them to undertake specific interactions with their environment. This requires versatile surface chemistries that can be manipulated to accommodate interactions with a variety of materials. Traditionally, high quality QDs are synthesized with hydrophobic organic capping agents such as trioctyl phosphine/trioctyl phosphine oxide (TOP/TOPO), which limit their interactions with specialized materials, particularly in aqueous environments. To overcome this limitation, several strategies have been implemented and involve coating the QD with amphiphilic phospholipids<sup>10</sup> and specialized polymers,<sup>11</sup> or performing a capping ligand exchange with thiol-containing organic acids including mercaptoacetic acid<sup>12</sup> or dihydrolipoic acid.<sup>13</sup> These water-stable QDs have been further modified by covalent<sup>12</sup> and

electrostatic attachment of antibodies,<sup>13,14</sup> proteins, and peptides for specific applications.

We have investigated the use of charge-driven polyelectrolyte coating of carboxylated ZnS capped CdSe QDs in aqueous solution to produce functionalized nanocrystals for device integration. While layer-by-layer deposition has been previously demonstrated on colloids,<sup>15</sup> microparticles,<sup>16,17</sup> and gold nanoparticle<sup>18</sup> surfaces, similar manipulation of semiconductor QDs has not been reported. Small size, high surface curvature, and difficult surface chemistries have made QD manipulation tedious and time consuming.<sup>19,20</sup> We coated anionic mercaptoacetic acid (MAA) treated QDs with cationic polyallylamine (PAA) and subsequently with polyvinylsulfonic acid (PVSA) (Figure 1a). The expected surface charge reversal is caused by excess polycation deposition due to overcompensation of charge neutralization.<sup>21</sup> This simple and robust technique chemically modifies QD surfaces by controlling the external surface charge and thickness of the deposited layers, as is characteristic of polyelectrolyte layer deposition.<sup>18</sup> It may allow integration of coated materials based on external surface chemistry, independent of the inorganic core. The modified QDs may be used as self-assembly blocks to build complex structures with oppositely charged materials, organized over multiple length scales. They may be tagged with biological or chemical species or interact with substrates to produce heterostructures. Here we explored the formation of charge-driven layer-by-layer<sup>22</sup> assemblies of cationic–anionic QD bilayers on

\* Corresponding author. Phone: (617) 324-2800. Fax: (617) 324-3300.  
E-mail: belcher@mit.edu.

<sup>†</sup> Department of Chemical Engineering.

<sup>‡</sup> Department of Materials Science and Engineering.

<sup>§</sup> Division of Biological Engineering.

<sup>||</sup> Institute for Soldier Nanotechnologies.

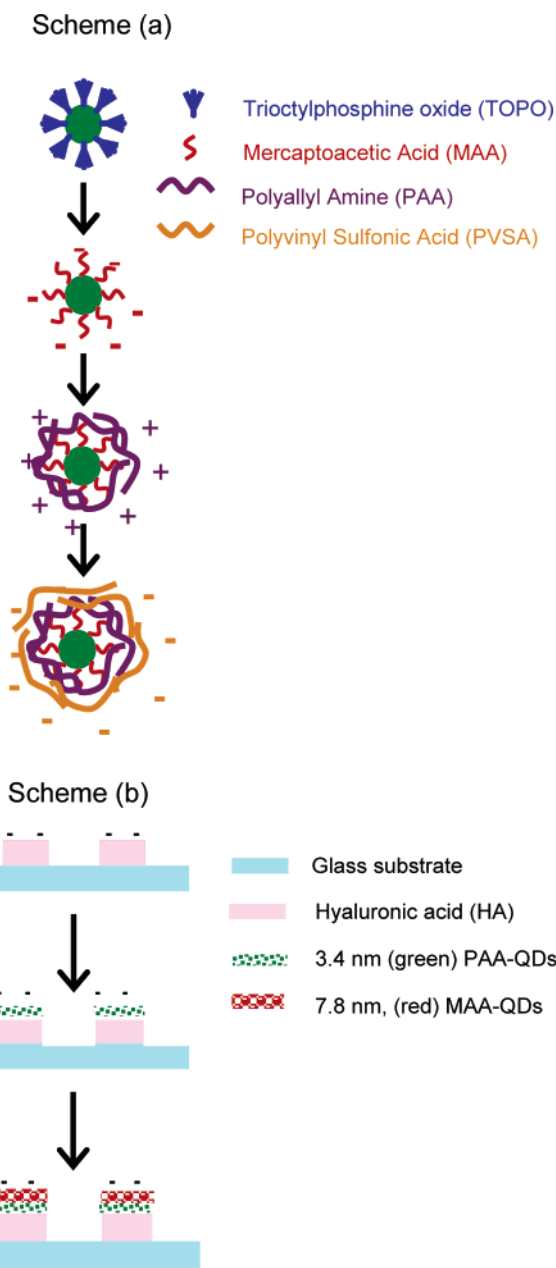


**Figure 1.** QD modification and patterning schemes. (a) The initial TOPO (hydrophobic) capping agent is replaced by a hydrophilic thiol-containing ligand (MAA) which renders the QDs negatively charged in water. Subsequent layers of positive (PAA) and negative (PVSA) polyelectrolytes are deposited on the QD surface, thereby modifying the surface charge. (b) Two-step, self-assembly scheme of modified QD on HA patterned glass substrates; anionic QD-MAA (green) adsorb to cationic QD-PAA (red), bound to HA patterns on nonadhesive glass (QD-MAA/QD-PAA/HA/glass).

anionic substrates (Figure 1b). Glass substrates were patterned with hyaluronic acid (HA), followed by the sequential deposition of cationic PAA-coated and anionic MAA-treated QDs to produce structured arrays. This was the first step toward demonstrating the feasibility of using polyelectrolyte-capped QDs to form highly structured materials for integration into devices.

ZnS-capped CdSe QDs (Evident Technologies) suspended in chloroform and excess MAA were briefly sonicated at 80 °C, resulting in displacement of the organic TOPO ligands

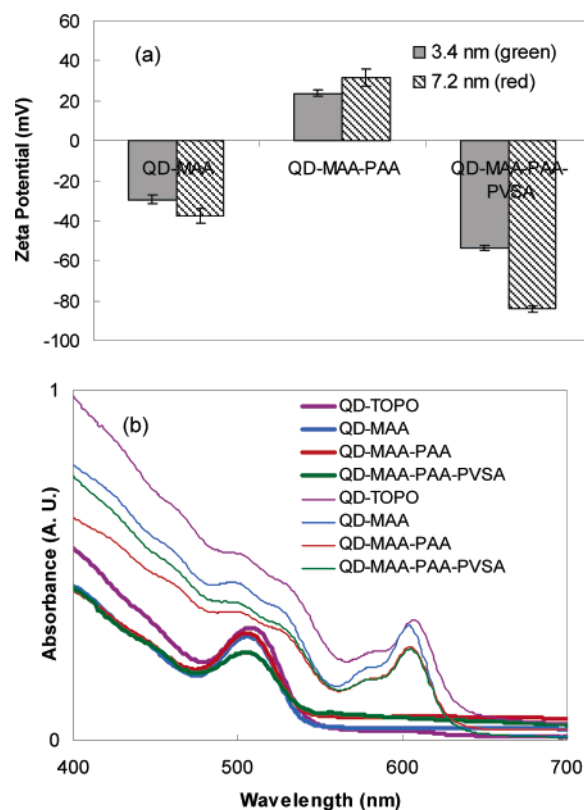


**Figure 2.** Characterizing modified QDs. (a) Zeta potentials of MAA-capped, PAA-coated, and PVSA-coated QDs in 50 mM NaCl. The solid bars represent the zeta potential of 3.4 nm (green) QDs, and the hatched bars represent those of 7.2 nm (red) ones. (b) Absorption spectra of unmodified (purple), MAA-modified (blue), PAA-coated (yellow), and PVSA-coated (orange) quantum dots. Heavy lines represent the spectra of 3.4 nm green quantum dots, while fine lines represent those of 7.2 nm red ones.

and rendering the QDs water soluble.<sup>12</sup> QD-MAA was purified twice by methanol/ethanol precipitation, centrifugation, and resuspension in 0.1 M, pH 9 tris buffer. Purified QD-MAA was mixed with excess 1 wt % PAA (16 kDa, Sigma) solution for 20 min, purified twice using Amicon separating columns (100 kDa, Millipore), and resuspended in tris buffer. Subsequent PVSA (7 kDa, Sigma) deposition and purification were carried out under the same conditions as PAA deposition, and final QD solutions were maintained at approximately 10 mg/mL, as determined by their optical density. QDs of two different sizes and emission peaks, 3.4 nm (green) and 7.2 nm (red), were modified.

Surface charge of the polyelectrolyte-coated QDs suspended in 50 mM NaCl in deionized water was determined using the Smoluchowski method (ZetaPals Analyzer), and the results are shown in Figure 2a. The solid bars represent the zeta potentials of modified 3.4 nm (green) QDs, while the hatched ones represent those of the 7.2 nm (red) QDs. The bare mercaptoacetic acid-modified QDs are  $-29.5$  mV (3.4 nm) and  $-37.5$  mV (7.2 nm), likely due to the presence of anionic MAA and hydroxyl molecules adsorbed to the dangling surface zinc ions.<sup>23</sup> The PAA-coated QDs are 23.6 mV (3.4 nm) and 31.6 mV (7.2 nm), while the PVSA-coated ones are  $-53.8$  mV (3.4 nm) and  $-84$  mV (7.2 nm). Both QD complexes show characteristic patterns of surface charge

reversals caused by excess polymer deposition due to overcompensation of charge neutralization.<sup>21</sup> These values are in agreement with those of other polyelectrolyte-coated colloidal systems found in the literature.<sup>18</sup> The absolute values of surface charges appear to be higher for the larger, 7.2 nm (red) QDs, particularly for the PVSA coat. This may be due to their lower surface curvature which allows the stiff polymer chains to fold around the nanoparticles more easily, and therefore facilitate polyelectrolyte adsorption.<sup>9</sup> This effect may be modulated by increasing the salt concentration to enhance polyelectrolyte deposition and result in thicker layers, as has been shown for other colloidal systems.<sup>18</sup>

The absorption spectra of the QD-MAA, PAA, PVSA (in tris buffer), and QD-TOPO (in DMSO) were obtained using a UV/vis spectrometer (Beckman Coulter, DU 800) and are shown in Figure 2b. For both the QDs (7.2 nm (red) and 3.4 nm (green)), the position of the first observable peak (607 and 508 nm, respectively) shifts slightly after MAA exchange, and remains blue shifted after polyelectrolyte adsorption. As expected, the dominant shifts for both modifications occur after MAA exchange, as previously reported. They are attributed to the differences in ligand binding affinities; the thiol-zinc bond is stronger than the TOPO-zinc bond and may cause distortion of the energy levels, leading to reorganization of the electronic density and increase in the confinement energy, thus resulting in a slight blue shift.<sup>24,25</sup> While photooxidation may also cause a blue shift, it is unlikely to be the cause since the peak positions and QD optical densities remained constant for several days post modification (data not shown). Other than peak position shifts, the overall shape of the spectra remained unchanged – there is no observable peak broadening which suggests that the structure of the QDs is preserved throughout the several processing steps and there is no clumping or fragmentation. Therefore, the polyelectrolyte deposition does not appear to be detrimental to the absorbance properties or size homogeneity of the QDs.

The size and morphology of the modified QDs were further investigated using transmission electron microscopy (TEM). The samples were prepared by adsorbing the nanoparticles on carbon-coated copper grid (Ladd Research Industries) for 20 min, drying, and imaging using a JEOL 2000FX at an accelerating voltage of 200 kV. The images in Figure 3 are the 7.2 nm (red) QD with (a) MAA, (b) PAA, and (c) PVSA coatings. The dense cores of the nanoparticles are approximately 7 nm in diameter, and their sizes and shapes do not vary after polyelectrolyte deposition. This reinforces that the QDs do not photooxidize or fragment due to polymer coating, and that the blue shifts in the absorption spectra (Figure 2b) are likely due to tighter thiol-zinc bonding. The QDs do not aggregate but remain distinct, which indicates that the polyelectrolytes form layers around individual particles. While the deposited layers are too thin to be visualized directly,<sup>26</sup> their presence is supported by the existence of a halo around the PVSA-coated QDs (Figure 3c) which is not visible in the MAA-treated QDs (Figure 3a). There is also an apparent increase in the interparticle

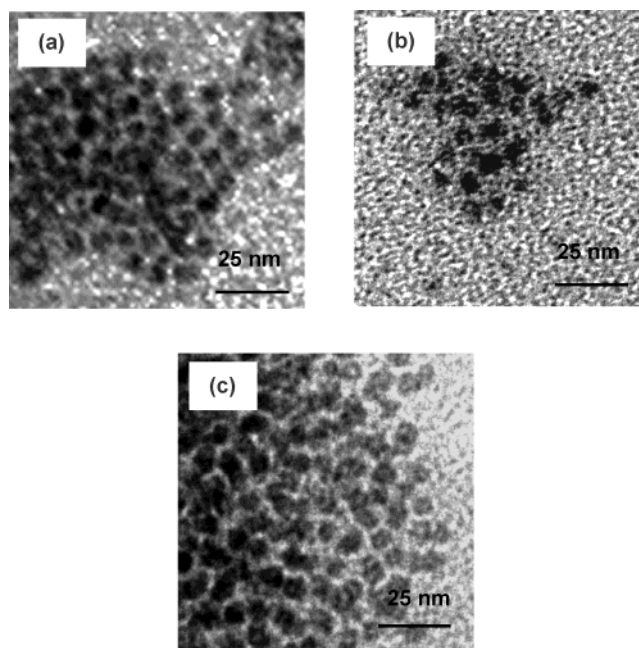


**Figure 3.** TEM images of modified 7.2 nm (red) QDs with (a) MAA, (b) PAA, and (c) PVSA surface coatings, at a magnification of 100 k.

spacing as additional polymer layers are deposited on the QD surface.

Layer-by-layer deposition of oppositely charged QDs on hyaluronic acid (HA) ( $M_n = 2.1$  MDa, Genzyme Inc.) patterned substrates was performed to demonstrate the specificity of electrostatic interactions. The HA patterned glass slides were prepared as described elsewhere.<sup>27,28</sup> Briefly, polydimethylsiloxane (PDMS) stamps were prepared by casting against silicon masters fabricated using photolithography. The stamps and the glass surfaces were both plasma cleaned for 2 min (model PDC-001, Harrick Scientific Inc.), the slides were spin coated (model CB 15, Headway Research, Inc.) with 5 mg/mL of HA and brought into conformal contact with the PDMS stamp. The HA was allowed to evaporate overnight before the stamp was peeled off, and freshly exposed patterned surfaces were washed three times by immersing in deionized water. A thin film of QD-PAA (cationic) was deposited on the substrate for 30 min, and excess QDs were removed by washing the substrate. A subsequent layer of QD-MAA (anionic) was similarly deposited on QD-PAA coated surfaces, and the sample washed and allowed to air-dry.

The patterned bilayer QD arrays were visualized using fluorescence and atomic force microscopy (AFM). Glass substrates with three layers were imaged: (i) patterned (anionic) HA layer adsorbed on glass, (ii) (cationic) PAA-coated 7.2 nm (red) QD layer electrostatically associated with the HA/glass substrate, and (iii) (anionic) MAA-treated 3.4 nm (green) QD layer assembled on the positive PAA-QD/HA/glass substrate. Fluorescence images were obtained using an Olympus microscope (IX51) with GFP (ex 450/40, em 525/50) and TRITC (ex 535/50, em 610/75) filters using SimplePCI software and are shown in Figures 4a and b, respectively. The AFM was operated in the tapping mode at

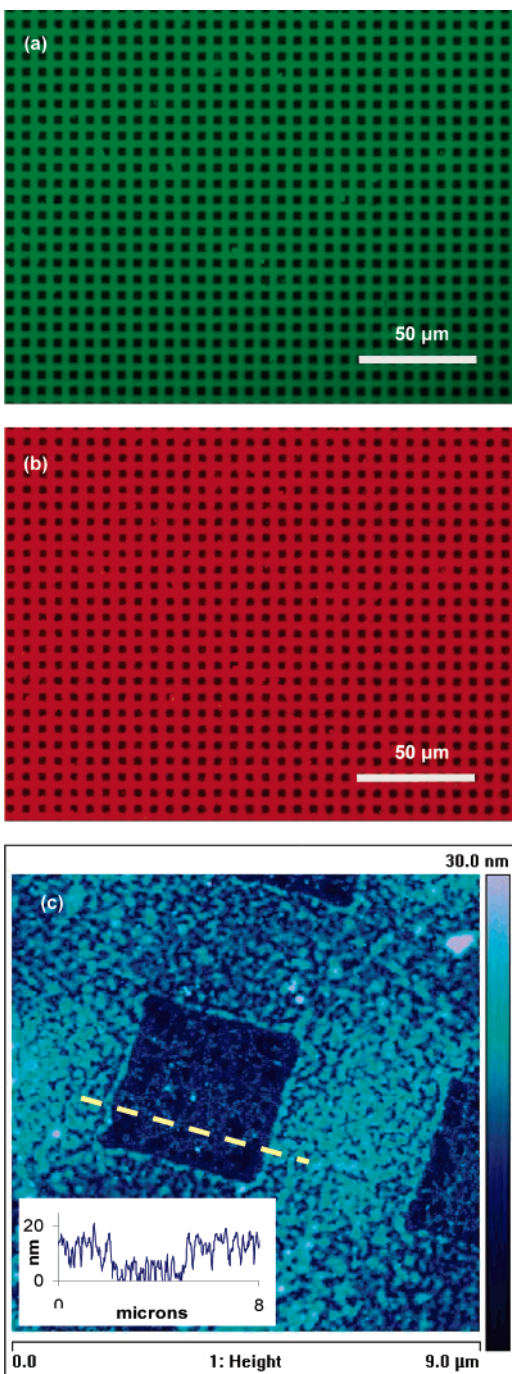


**Figure 4.** Images of patterned QDs. The HA-patterned glass substrate has a bilayer of cationic (PAA) 7.2 nm (red) and anionic (MAA) 3.4 nm (green) QDs deposited sequentially (QD-MAA/QD-PAA/HA/glass). Figures (a) and (b) are the fluorescence images of the same region viewed using the green (GFP) and red (TRITC) filters, respectively. Figure (c) is an AFM image of the bilayered structure, and the height profile across the dotted line is shown in the inset.

a scan rate of 0.5 Hz using 300 kHz (MikcoMasch) tips. Images were taken on a Nanoscope IV (Digital Instruments) and data was manipulated using Nanoscope VI software (Veeco Instruments Inc.); the final image and height profile are shown in Figure 4c.

The patterned bilayer images show excellent overlap between the green anionic 3.4 nm (Figure 4a) and red

cationic 7.2 nm (Figure 4b) QD layers. The fluorescent areas are where QD binding has occurred and the dark squares correspond to the nonadhesive glass surface. The modified QDs selectively adhere to oppositely charged substrates but not to the untreated glass, and do not wash off even after several rinses. The electrostatic forces are strong enough to enable QD assembly on oppositely charged polyelectrolyte (HA) and QD surfaces, even after washing. The films appear smooth and show conformal coverage with very little clumping or pattern distortion, even after drying. The pattern fidelity is very high: the features have sharp edges, the layers are precisely aligned, and the patterns are reproducible over large areas.

AFM images of the patterned bilayers were obtained to further characterize the feature integrity and the height profiles, as shown in Figure 4c. The features appear to be the same size (3  $\mu\text{m}$  squares) with an aspect ratio close to unity. There is some nonspecific adsorption on the untreated glass surface, which could be due to the residual debris from the PDMS mold or the polyelectrolytes. The height difference between the bilayer and the nonadhering regions, as indicated by the height profile (inset), is approximately 15 nm. The HA layer is approximately 3–6 nm in height<sup>27,28</sup> while the PAA- and MAA-modified QDs are approximately 7 and 3 nm respectively, which implies that monolayers of each quantum dot may be deposited on the surface. It may be possible to control the layer thickness and deposit additional layers, depending on the salt concentration.<sup>18</sup>

In conclusion, this paper investigates the polyelectrolyte layer-by-layer modification of QDs and their application to produce structured heterostructures. The modified QDs displayed the characteristic surface charge reversal as monitored by the zeta potential, while the absorbance properties remained largely unchanged. TEM results revealed that the QDs neither aggregated nor fragmented and were individually coated with the polyelectrolyte shells. These charged nanoparticles were capable of forming multi-QD, self-assembled arrays on patterned substrates, as revealed by fluorescence and atomic force microscopy. Since the self-assembly is independent of the inorganic core material, this approach should be easily adapted to pattern multicomposition nanoparticles to form ordered heterostructures. Thus we have demonstrated a technique for manipulating quantum dot surface chemistries and directed spatial organization for integration into potential devices, probes, and sensors.

**Acknowledgment.** The authors thank Andre Ditsch for his insightful discussions about obtaining zeta potentials, and Professor Alan Hatton for allowing generous use of his zeta potential analyzer. Graduate student support was provided in part by the EDAAD scholarship, administered through The Executive Office (United Arab Emirates). This research was supported in part by the David and Lucille Packard Foundation, the National Science Foundation Nanotechnologies Interdisciplinary Research Team, and the U.S. Army through the Institute for Soldier Nanotechnologies, under contract DAAD-19-02D-0002 with the U.S. Army Research Office. The content does not necessarily reflect the position of the government, and no endorsement should be inferred.

## References

- (1) Murray, C. B.; Kagan, C. R.; Bawendi, M. G. *Annu. Rev. Mater. Sci.* **2000**, *30*, 545.
- (2) Nozik, A. J. *Physica E* **2002**, *14*, 115.
- (3) Coe, S.; Woo, W. K.; Bawendi, M. G.; Bulovic, V. *Nature* **2002**, *420*, 800.
- (4) Baron, T.; Fernandes, A.; Damlencourt, J. F.; De Salvo, B.; Martin, F.; Mazen, F.; Haukka, S. *Appl. Phys. Lett.* **2003**, *82*, 4151.
- (5) Han, M. Y.; Gao, X. H.; Su, J. Z.; Nie, S. *Nature Biotechnol.* **2001**, *19*, 631.
- (6) Alivisatos, A. P. *Nature Biotechnol.* **2004**, *22*, 47.
- (7) Alivisatos, A. P. *Science* **1996**, *271*, 933.
- (8) Clapp, A. R.; Medintz, I. L.; Mauro, J. M.; Fisher, B. R.; Bawendi, M. G.; Mattoussi, H. *J. Am. Chem. Soc.* **2004**, *126*, 301.
- (9) Caruso, F. *Adv. Mater.* **2001**, *13*, 11.
- (10) Dubertret, B.; Skourides, P.; Norris, D. J.; Noireaux, V.; Brivanlou, A. H.; Libchaber, A. *Science* **2002**, *298*, 1759.
- (11) Wu, X. Y.; Liu, H. J.; Liu, J. Q.; Haley, K. N.; Treadway, J. A.; Larson, J. P.; Ge, N. F.; Peale, F.; Bruchez, M. P. *Nature Biotechnol.* **2003**, *21*, 41.
- (12) Chan, W. C. W.; Nie, S. M. *Science* **1998**, *281*, 2016.
- (13) Mattoussi, H.; Mauro, J. M.; Goldman, E. R.; Anderson, G. P.; Sundar, V. C.; Mikulec, F. V.; Bawendi, M. G. *J. Am. Chem. Soc.* **2000**, *122*, 12142.
- (14) Sukhanova, A.; Devy, M.; Venteo, L.; Kaplan, H.; Artemyev, M.; Oleinikov, V.; Klinov, D.; Pluot, M.; Cohen, J. H. M.; Nabiev, I. *Anal. Chem.* **2004**, *324*, 60.
- (15) Chodanowski, P.; Stoll, S. J. *J. Chem. Phys.* **2001**, *115*, 4951.
- (16) Zheng, H. P.; Lee, I.; Rubner, M. F.; Hammond, P. T. *Adv. Mater.* **2002**, *14*, 569.
- (17) Lee, I.; Zheng, H. P.; Rubner, M. F.; Hammond, P. T. *Adv. Mater.* **2002**, *14*, 572.
- (18) Mayya, K. S.; Schoeler, B.; Caruso, F. *Adv. Funct. Mater.* **2003**, *13*, 183.
- (19) Salgueirino-Maceira, V.; Caruso, F.; Liz-Marzan, L. M. *J. Phys. Chem. B* **2003**, *107*, 10990.
- (20) Stoll, S.; Chodanowski, P. *Macromolecules* **2002**, *35*, 9556.
- (21) Decher, G. *Science* **1997**, *277*, 1232.
- (22) Xia, Y. N.; Whitesides, G. M. *Angew. Chem., Int. Ed.* **1998**, *37*, 551.
- (23) O'Neil, M.; Marohn, J.; McLendon, G. *J. Phys. Chem.* **1990**, *94*, 4356.
- (24) Talapin, D. V.; Rogach, A. L.; Kornowski, A.; Haase, M.; Weller, H. *Nano Lett.* **2001**, *1*, 207.
- (25) Wuister, S. F.; Swart, I.; van Driel, F.; Hickey, S. G.; Donega, C. D. *Nano Lett.* **2003**, *3*, 503.
- (26) Kato, N.; Schuetz, P.; Fery, A.; Caruso, F. *Macromolecules* **2002**, *35*, 9780.
- (27) Suh, K. Y.; Khademhosseini, A.; Yang, J. M.; Tran, T. T.; Eng, G.; Langer, R. *Adv. Mater.* **2004**, *16*, 584.
- (28) Khademhosseini, A.; Suh, K. Y.; Yang, J. M.; Eng, G.; Yeh, J.; Levenberg, S.; Langer, R. *Biomaterials* **2004**, *25*, 3583.

NL0493287